Proc. Natl. Acad. Sci. USA
Vol. 93, pp. 9588–9593, September 1996
Cell Biology

Forced expression of the tumor suppressor adenomatosis polyposis coli protein induces disordered cell migration in the intestinal epithelium

(catenins/E-cadherin/embryonic stem cells/chimeric mice)

MELISSA H. WONG, MICHELLE L. HERMISTON, ANDREW J. SYDER, AND JEFFREY I. GORDON*

Department of Molecular Biology and Pharmacology, Washington University School of Medicine, St. Louis, MO 63110

Communicated by David M. Kipnis, Washington University School of Medicine, St. Louis, MO, June 13, 1996 (received for review April 19, 1996)

ABSTRACT **Mutations of the human adenomatosis polyposis coli (*APC*) gene are associated with the development of familial as well as sporadic intestinal neoplasia. To examine the *in vivo* function of APC, 129/Sv embryonic stem (ES) cells were transfected with DNA encoding the wild-type human protein under the control of a promoter that is active in all four of the small intestine's principal epithelial lineages during their migration-associated differentiation. ES-APC cells were then introduced into C57BL/6-ROSA26 blastocysts. Analyses of adult B6-ROSA26 ↔ 129/Sv-APC chimeric mice revealed that forced expression of APC results in markedly disordered cell migration. When compared with the effects of forced expression of E-cadherin, the data suggest that APC–catenin and E-cadherin–catenin complexes have opposing effects on intestinal epithelial cell movement/adhesiveness; augmentation of E-cadherin–β-catenin complexes produces a highly ordered, "adhesive" migration, whereas augmentation of APC–β-catenin complexes produces a disordered, nonadhesive migratory phenotype. We propose that APC mutations may promote tumorigenesis by increasing the relative activity of cadherin–catenin complexes, resulting in enhanced adhesiveness and functional anchorage of initiated cells within the intestinal crypt. Our studies also indicate that chimeric mice generated from B6-ROSA26 blastocysts and genetically manipulated ES cells should be useful for auditing gene function in the gastrointestinal tract and in other tissues.**

The human adenomatosis polyposis coli (*APC*) gene encodes a 2844 amino acid protein (1). Mutations in *APC* are an early event in the development of sporadic human colorectal tumors. They also cause familial adenomatosis polyposis, a disorder with a dominant mode of inheritance that results in the development of hundreds or even thousands of colorectal adenomas within the first 20–30 years of life, ultimately leading to adenocarcinoma (1–4). *APC* mutations are also associated with Gardner syndrome (intestinal adenomas, osteomas, dental abnormalities, soft-tissue tumors, and retinal pigment epithelial hypertrophy) and medulloblastomas (Turcot syndrome) (5, 6). A Leu^{850} → stop mutation of the mouse *Apc* gene (Apc^{Min}) produces intestinal adenomas, desmoid tumors, mammary adenocarcinomas, and mammary keratoacanthomas in adult animals (7–9). Mice homozygous for Apc^{Min} exhibit early embryonic lethality, establishing an essential role for the wild-type protein in development (10).

The function of APC has not been defined *in vivo*. Several recent observations suggest that APC may affect cell adhesion and/or migration. Forced expression of wild-type APC (APC^{Wt}) in kidney and colonic epithelial cell lines results in its association with microtubules (11, 12). The C terminal third of APC, which is typically deleted in colorectal carcinomas (4), is needed for microtubular association and is sufficient to promote microtubule assembly and bundling *in vitro* (4, 11, 12). APC may influence adhesion through its interactions with catenins. β-catenin binds to the highly conserved cytoplasmic domain of E-cadherin (13, 14), the principal intestinal epithelial cadherin (15). Once formed, cadherin–β-catenin complexes are able to affiliate with α-catenin, which functions to link them to the actin cytoskeleton, resulting in productive cell adhesion (14, 16, 17). APC also forms complexes with β-catenin and α-catenin (18–20). Formation and stabilization of APC–β-catenin complexes are modulated by components of the *wingless/Int* (Wnt) signal transduction pathway (21, 22). The physiologic functions of APC–catenin complexes are unknown. However, these complexes appear to exist in equilibrium with free β-catenin and with cadherin–β-catenin complexes (20–22). Expression of APC^{Wt} in a human colon carcinoma cell line has been shown to perturb this equilibrium (23).

The adult mouse small intestinal epithelium is a good system to study cell adhesion and migration. Maintenance of tight cell–cell adhesion is essential for the epithelium to function as an effective biological barrier. The epithelium also undergoes continuous and rapid self-renewal through an orderly migration-associated differentiation of its component lineages. Cellular proliferation is confined to crypts that surround the base of each intestinal villus. Postmitotic absorptive enterocytes, mucus-producing goblet cells, and enteroendocrine cells exit the crypt, complete their differentiation as they move up adjacent villi in vertical coherent columns, enter a death program, and are exfoliated at the villus tip. The sequence is recapitulated every 3–5 days (for review, see ref. 24). Paneth cells produce antimicrobial peptides and growth factors, differentiate as they migrate downward to the crypt base, and are eliminated by phagocytosis (25).

In this report, we describe the use of chimeric transgenic mice to define the effects of forced expression of human APC^{Wt} on intestinal epithelial cell adhesion and migration.

MATERIALS AND METHODS

Generation of Chimeric Transgenic Animals. A full-length 8.9-kb human APC cDNA flanked by *Bam*HI sites (a gift from Ken Kinzler, Johns Hopkins University, Baltimore) was subcloned into the unique *Bam*HI site present in $pL596hGH\Delta B_2$ (26, 27), yielding pLAPC. This placed the APC cDNA at nucleotide +3 of the human growth hormone (hGH) gene and under the control of nucleotides −596 to +21 of a rat fatty acid binding protein gene (*Fabpl*). The *Fabpl–APC–hGH–pgk*neo

The publication costs of this article were defrayed in part by page charge payment. This article must therefore be hereby marked "*advertisement*" in accordance with 18 U.S.C. §1734 solely to indicate this fact.

Abbreviations: APC, adenomatous polyposis coli; ES cells, embryonic stem cells.

*To whom reprint requests should be addressed at: Department of Molecular Biology and Pharmacology, Box 8103, Washington University School of Medicine, 660 South Euclid Avenue, St. Louis, MO 63110. e-mail: jgordon@pharmdec.wustl.edu.

insert from pLAPC was excised with *Sac*I and *Xba*I, purified, and electroporated into D3 embryonic stem (ES) cells (15).

129/Sv ROSA26 mice (ref. 28; obtained from Phil Soriano, Fred Hutchinson Cancer Research Center, Seattle) were backcrossed to C57BL/6 (B6) mice (The Jackson Laboratory) for four generations. Six independent D3-APC cell lines were injected into B6-ROSA26 blastocysts (≈10-15 cells per blast) to generate B6-ROSA26 ↔ 129/Sv-APC chimeras. Control B6-ROSA26 ↔ 129/Sv mice were produced using nontransfected D3 ES cells.

All animals were maintained in microisolator cages and given Pico Lab Rodent Diet 20 (PMI Feeds, St. Louis) ad libitum. Routine screens for hepatitis, minute, lymphocytic choriomeningitis, ectromelia, polyoma, sendai, pneumonia, and adenoviruses, enteric bacterial pathogens, and parasites were negative.

Staining Whole Mounts of the Intestine. The small intestine and colon were removed *en bloc* from mice immediately after they were killed, flushed with phosphate-buffered saline (PBS) followed by periodate-lysine-paraformaldehyde (PLP; ref. 29), opened with a longitudinal incision, pinned, fixed in PLP for 1 h at 24°C, washed in PBS, incubated in 20 mM DTT, 20% ethanol, and 150 mM Tris·HCl (pH 8.0) for 45 min to remove mucus, washed again in PBS, and then placed in a solution of PBS containing 2 mM 5-bromo-4-chloro-3-indolyl β-D-galactoside (X-Gal; Boehringer Mannheim), 4 mM each potassium ferricyanide and ferrocyanide, and 2 mM $MgCl_2$ (final pH 7.6) for 12 h at 4°C. Staining with Bluo-Gal was performed using a protocol described by its manufacturer (Life Technologies, Grand Island, NY). For double labeling, X-Gal- or Bluo-Gal-stained whole mounts were subsequently incubated for 12 h at 4°C with peroxidase-conjugated *Ulex europaeus* agglutinin type 1 (UEA1, Sigma; 5 μg/ml in lectin blocking buffer; ref. 15). The bound lectin was visualized using previously described methods (15).

Immunohistochemistry. Protocols used for single and multilabel immunohistochemical studies were as described (15, 30). PLP-fixed, paraffin-embedded sections were incubated with sheep anti-human lysozyme (Dako), rabbit anti-mouse cryptdin-1 (obtained from M. Selsted, University of California, Irvine; ref. 25), sheep anti-mouse IgA (Sigma; ref. 27), and rat anti-mouse β_7 integrin (PharMingen; ref. 27). PLP-fixed, frozen sections were incubated with affinity-purified rabbit α-catenin antibodies (ref. 31; kindly provided by Inke Näthke and James Nelson, Stanford University, Stanford, CA) or affinity-purified rabbit antibodies raised against amino acids 1034–2130 of human APC (APC2; ref. 12; a gift from Paul Polakis, Onyx Pharmaceuticals, Richmond, CA). The cellular and intracellular distributions of E-cadherin and β-catenin were defined using tissue that had been embedded in OCT (Miles), submerged in Cytocool freezing media (Baxter) at −80°C, sectioned in a Cryostat (section thickness, 6–8 μm), fixed in ice-cold methanol for 10 min, and rehydrated in PBS. The fresh frozen sections were then incubated either with previously characterized rat E-cadherin monoclonal antibodies (the preparation described in ref. 32 was generously supplied by Rolf Kemler, Max Planck Institute for Immunobiology, Germany; DECMA-1 mAb was purchased from Sigma) or with rabbit anti-β-catenin sera (ref. 31, from I. Näthke and J. Nelson; also see refs. 27 and 30). 129/Sv cells in these fresh frozen sections were genotyped using peroxidase-conjugated UEA1.

Confocal Microscopy. Stained sections (see above) were viewed with a Molecular Dynamics model 2001 confocal microscope. Scans were performed at 1 μm intervals.

Quantitation of Mitosis and Apoptosis. Comparably aged normal B6-ROSA26 ↔ 129/Sv and chimeric transgenic B6-ROSA26 ↔ 129/Sv-APC^{Wt} mice were killed. The middle third (jejunum) of Bluo-Gal-stained small intestine was embedded in paraffin. Serial sections (5 μm thick) were generated and stained with hematoxylin and eosin. M phase and apoptotic cells were counted in well-oriented intact crypt-villus units located in adjacent B6 and 129/Sv patches (30, 33) ($n = 2$ mice per cell line; 100 crypt-villus units per genotype per mouse). The position of each M phase or apoptotic cell was noted: (*i*) crypts were subdivided into lower, middle, and upper thirds and (*ii*) the villus was considered as a single entity (30). Data obtained from B6-ROSA and 129/Sv crypt-villus units were analyzed using Student's *t* test (SigmaPlot).

RESULTS AND DISCUSSION

A Dual-Marker System for Genotyping Intestinal Epithelial Cell Populations in Chimeric Mice. The features of this system are illustrated in Fig. 1. Normal or genetically manipulated 129/Sv ES cells (see below) were introduced into B6-ROSA26 blastocysts. ROSA26 is an ES cell line identified during an enhancer trap experiment that used the bacterial lacZ gene as a reporter (28). 129/Sv mice derived from this cell line express lacZ throughout their crypt-villus and gastric-colonic axes. Reporter expression in the gut is sustained from the time the intestinal epithelium undergoes cytodifferentiation (initiated on embryonic day 15) through completion of crypt-villus morphogenesis (postnatal day 21), and for at least the first 18 months of postnatal life (data not shown). This pattern of lacZ expression is not affected when 129/Sv-ROSA26 mice are backcrossed to C57BL/6 animals for four to eight generations.

The small intestine of adult B6-ROSA26 ↔ 129/Sv chimeras contains patches of 129/Sv crypt-villus units and patches of B6 crypt-villus units. B6-ROSA26 patches can be identified by staining whole mount preparations with X-Gal (Fig. 1*A*). 129/Sv patches appear white. Patches can also be genotyped based on their differing patterns of lectin binding: 129/Sv but not B6 enterocytes bind the Fucα1,2Galβ-specific lectin *Ul. europaeus* agglutinin type 1 (Fig. 1*B*). All crypts in each patch are monoclonal, i.e., they are populated by either B6-ROSA26 or 129/Sv cells but not by a mixture of both (Fig. 1*C*). There are several advantages of using this dual-marker system. The carbohydrate polymorphism recognized by UEA1 cannot be used to genotype crypts (Fig. 1*C*), is only expressed after postnatal day 21, is limited to the small intestine, and may be affected by genetic manipulations that perturb the state of enterocytic differentiation. In contrast, the lacZ marker can be used to genotype the embryonic intestinal epithelium, small intestinal crypts, and the colonic epithelium (Fig. 1 *C–E*).

The dual-marker system can also be used for defining defects in cell migration. Polyclonal villi, positioned at the boundaries of B6 and 129/Sv patches, contain cellular contributions from monoclonal 129/Sv crypts and monoclonal B6-ROSA26 crypts. These polyclonal villi appear striped when stained with X-Gal (or Bluo-Gal) and UEA1: vertical coherent columns of $UEA1^+$ 129/Sv cells are juxtaposed next to vertical coherent columns of $lacZ^+$ B6 cells (Fig. 1 *F* and *G*). Disruption of cell migration pathways could be identified by noting whether the polyclonal villi contain coherent columns of cells composed of a single genotype, whether the boundaries between columns are sharp, or whether there is a mixing of blue $lacZ^+$ and $UEA1^+$ cells throughout the villus.

The Normal Distribution of APC Along the Crypt-Villus Axis. A well-characterized preparation of affinity-purified rabbit antibodies, raised against amino acids 1034–2130 of human APC (12), was used to define the distribution of mouse APC in normal B6-ROSA26 ↔ 129/Sv chimeras (i.e., control mice generated using nontransfected ES cells). APC levels increase markedly at the crypt-villus junction (Fig. 1*H*), a result similar to that reported recently by Miyashiro and coworkers (34). Expression is sustained as cells complete their upward migration to the villus tip and is also evident in differentiated Paneth cells located at the crypt base (Fig. 1*H*). Confocal microscopy disclosed that APC is distributed at the

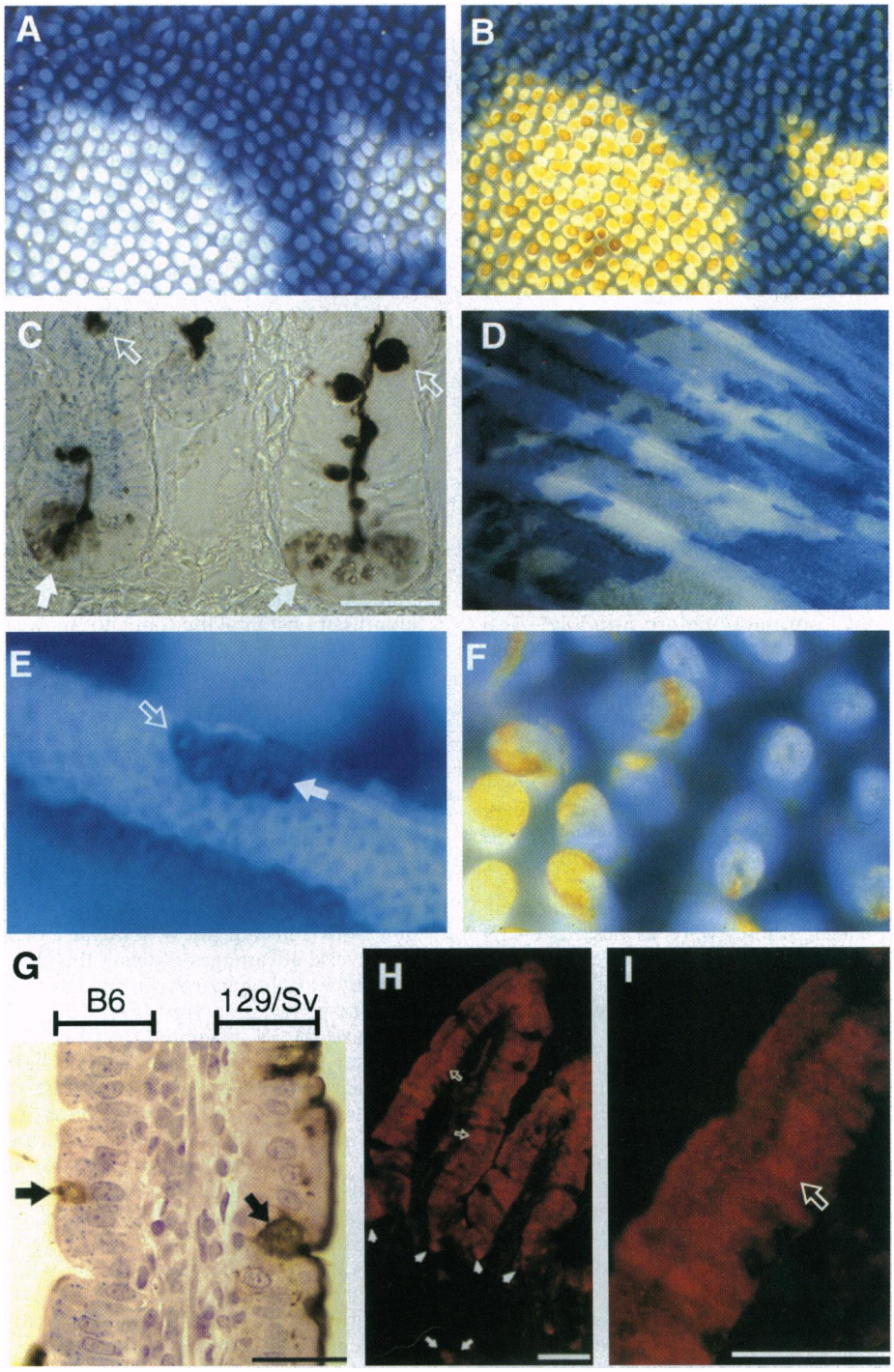

FIG. 1. A dual marker system for genotyping cells in adult B6-ROSA26 ↔ 129/Sv mouse intestinal epithelium. (*A*) Nontransfected 129/Sv ES cells were used to generate "normal" B6-ROSA 26 ↔ 129/Sv chimeras. A whole mount of jejunum stained with X-Gal is shown. The white patches of lacZ$^-$ crypt-villus units are 129/Sv; the blue lacZ$^+$ crypt-villus units are B6-ROSA26. (*B*) The same whole mount as in *A*, lightly stained with peroxidase-conjugated UEA1 (visualized with 3′,3-diaminobenzidine). 129/Sv villus enterocytes bind the lectin and appear yellow-brown. (*C*) Section prepared from a whole mount processed as in *B* but with lacZ visualized using Bluo-Gal. Two adjacent crypts are shown. The monoclonal B6-ROSA crypt on the left is composed of a wholly blue punctate-stained population of lacZ-expressing epithelial cells. The 129/Sv crypt on the right is entirely lacZ$^-$. Peroxidase-UEA1 (brown) binds to Paneth cells located at the base of both crypts (solid arrows) and to goblet cells (open arrows). (*D*) X-Gal stained whole mount preparation from the midportion of a B6-ROSA26 ↔ 129/Sv colon. The colonic epithelium has a folded appearance and is composed of patches of lacZ$^-$ 129/Sv cells and dark blue lacZ$^+$ B6-ROSA26 cells. (*E*) High power view of the preparation shown in *D*. The colon lacks villi. Cells exit each crypt and form a flat, surface epithelial cuff that surrounds its orifice (e.g., solid arrow). Note the sharp margin between the cluster of B6-ROSA crypt units and the surrounding patch of 129/Sv units. An open arrow points to one such B6-ROSA26 cuff. The absence of segmentation of this cuff with wedges or clusters of lacZ$^-$ (light blue-white) 129/Sv cells indicates that the colonic cuffs are not polyclonal but rather are each populated by cells derived from a single underlying monoclonal crypt. (*F*) Jejunal polyclonal villi processed as in *B*. These villi are supplied by monoclonal B6-ROSA26 and 129/Sv crypts. Vertical coherent columns of blue lacZ$^+$/UEA1$^-$ B6-ROSA26 epithelial cells are juxtaposed next to vertical coherent columns of yellow-brown lacZ$^-$/UEA$^+$ 129/Sv cells. (*G*) Section of a jejunal polyclonal villus prepared from a whole mount stained with Bluo-Gal, peroxidase-UEA1, and counterstained with hematoxylin and eosin. LacZ$^-$ 129/Sv enterocytes do not exhibit the punctate blue staining seen in B6 cells but do bind peroxidase-conjugated (*Legend continues on the opposite page.*)

periphery of villus epithelial cells where it appears to form small granular aggregates (Fig. 1*I*). Immunoreactive protein is also present throughout the cytoplasm and in the nucleus (Fig. 1*I*). The nuclear location is interesting in light of APC's proposed function as a regulator/effector of *wingless*/Wnt signaling (refs. 21 and 22; for review, see ref. 35). There are no apparent differences in the intracellular distributions or levels of APC in adjacent B6 and 129/Sv crypt-villus units (data not shown).

Forced Expression of APC^{Wt} Results in Disordered Cell Migration. D3 129/Sv ES cells were stably transfected with the entire human APC^{Wt} open reading frame under the control of a fatty acid binding protein gene promoter (*Fabpl*). This promoter has been extensively characterized in transgenic and chimeric transgenic mice (26, 27, 30, 36, 37) and shown to direct foreign gene expression along the entire length of the crypt-villus and duodenal-ileal axes. The promoter is active from embryonic day 15 through at least the first 2 years of life. Reporter expression is initiated in proliferating crypt epithelial cells and is sustained as all four lineages complete their migration-associated differentiation (36). Highest levels of *Fabpl*-reporter expression occur in the jejunum.

Nontransfected D3- and six independent, stably transfected D3-ES cell lines were each injected into B6-ROSA26 blastocysts. The resulting specific-pathogen-free chimeric mice were examined at 1.5 and 7 months of age (n = 1–4 mice per cell line per time point; percent 129/Sv contribution to coat color = 20–80%).

There were no statistically significant differences in body weights between comparably aged normal and B6-ROSA26 ↔ 129/Sv-APC chimeras with equivalent degrees of 129/Sv contribution. However, each of the six 129/Sv-APC ES cell lines produced B6-ROSA26 ↔ 129/Sv-APC mice with the same distinctive phenotype. Polyclonal villi contained intermingled populations of lacZ$^+$B6 and UEA1$^+$129/Sv cells rather than coherent vertical columns of cells of the same genotype (Fig. 2 *A* and *B*). Movement of 129/Sv-APC epithelial cells into B6 columns was not accompanied by any detectable change in villus height or morphology. Perturbations in the orderliness of cell migration were greatest in the jejunum. Paneth cells (defined by UEA1 plus antibodies to lysozyme and cryptdins; ref. 25) were confined to the crypt base, indicating that their downward migration was not disrupted (data not shown).

The ability to examine the interface between 129/Sv-APC and B6 cells in polyclonal villi was critical for defining the disordered movement. This abnormality was masked in villi composed entirely of 129/Sv-APC cells: their epithelium appeared normal when stained with UEA1 (Fig. 2 *C* and *D*).

Immunohistochemical studies confirmed that UEA1$^+$ 129/Sv-APC epithelial cells had increased levels of APC, although the protein's intracellular distribution was not appreciably altered (Fig. 2 *E* and *F*). Forced expression of APC had no detectable effect on the cellular distributions or levels of α-catenin (Fig. 2 *G* and *H*), β-catenin (Fig. 2 *I* and *J*), or E-cadherin (Fig. 2*K*).

No physical disruptions of cell–cell or cell–substratum contacts were detectable in the B6-ROSA26 ↔ 129/Sv-APC intestinal epithelium by light microscopy (Fig. 2 *E–K*). In addition, the chimeric transgenic animals had no evidence of functional disruptions in their mucosal barrier. There were no increases in B_7 integrin-positive intraepithelial lymphocytes or inflammatory responses in the underlying lamina propria (defined by staining sections with hematoxylin and eosin and with antibodies to IgA) (data not shown).

The disordered migration phenotype noted in B6-ROSA26 ↔ 129/Sv-APC chimeras contrasts with the phenotype produced by forced expression of E-cadherin using the same *Fabpl* promoter (30). Augmentation of cellular E-cadherin pools in B6 ↔ 129/Sv-ECAD mice slows epithelial migration up the crypt-villus unit but does not affect the orderliness of movement nor does it result in detectable changes in the intracellular distributions of α- or β-catenin (30). The number and width of 129/Sv-ECAD stripes in B6 ↔ 129/Sv-ECAD polyclonal villi are not reduced or attenuated despite the more rapid movement of B6 cells (30). These findings lead to the hypothesis that a shift toward E-cadherin–β-catenin complex formation produces a highly ordered, highly "adhesive" migration, whereas augmentation of APC–β-catenin complexes produces a disordered, nonadhesive ("invasive") migratory phenotype.

The fact that 129/Sv-APC^{Wt} cells can enter columns of normal B6 cells in polyclonal villi suggests that migration along the crypt-villus axis is not a simple "passive" response to cell production in the crypt but rather an actively regulated process. The preservation of the normal downward migration of 129/Sv-APC Paneth cells to the crypt base contrasts with the disordered upward migration of the enterocytic (and goblet cell) lineages. The mechanisms that underlie the "decision" of Paneth cells to move down, rather than up, the crypt are not known. Our data suggest that the decision and its execution are not sensitive to the effects of APC.

Forced Expression of APC^{Wt} Has no Detectable Effect on Proliferative Status or Apoptosis. We examined the effects of forced expression of APC^{Wt} on cellular proliferation and death programs for two reasons. First, a recent report indicated that forced expression of the protein in NIH 3T3 cells blocks progression from G_1 to S (38). This effect is inhibited by C-terminal truncation mutants, perhaps through formation of heterodimers with APC^{Wt} via their intact N-terminal domains (39), thereby allowing the mutants to function in a dominant negative manner (4). Second, *Fabpl*-directed augmentation of cellular E-cadherin pools in B6 ↔ 129/Sv-ECAD mice is associated with a decrease in proliferation and an increase in apoptosis within 129/Sv-ECAD crypts (but not their associated villi) (30).

There were no statistically significant differences in the number of M phase or apoptotic cells in the adjacent B6-ROSA26 and 129/SV jejunal crypts of normal B6-ROSA26 ↔ 129/Sv or B6-ROSA26 ↔ 129/Sv-APC mice (data not shown). Forced expression of APC^{Wt} does not result in a return of postmitotic villus epithelial cells to the cell cycle or produce a statistically significant increase in their apoptosis (data not shown).

These data establish that the disordered migration phenotype noted on the villus is not associated with a phenomenon akin to anoikis. The latter term refers to the apoptosis associated with disruption of integrin-mediated cell–cell or cell–matrix contacts (40, 41).

Prospectus. The ability to influence cell movement is likely to have a profound effect on tumorigenesis in the self-renewing intestinal epithelium, where rapid cell loss represents a convenient and efficient way of eliminating cells that have acquired mutations. Initiation of tumorigenesis in the intestine

UEA1 (brown) to their apical membranes. A subset of B6-ROSA26 and 129/Sv goblet cells produce fucosylated glycoconjugates recognized by UEA1 (arrows). (*H*) Section of a B6-ROSA26 patch of jejunum incubated with affinity purified rabbit anti-APC (visualized with Cy3-donkey anti-rabbit Ig). APC levels rise abruptly at crypt-villus junctions (denoted by solid arrowheads) and are sustained as epithelial cells complete their migration up the villus. APC is located in the nucleus (e.g., open arrow) and in the cytoplasm of these cells. Paneth cells positioned at the crypt base (closed arrows) are also prominently stained. (*I*) Confocal micrograph of the jejunal villus in *H*. Nuclear staining is evident (e.g., open arrow) as is the clumping of immunoreactive APC in the cytoplasm. (Bars = 25 μm.)

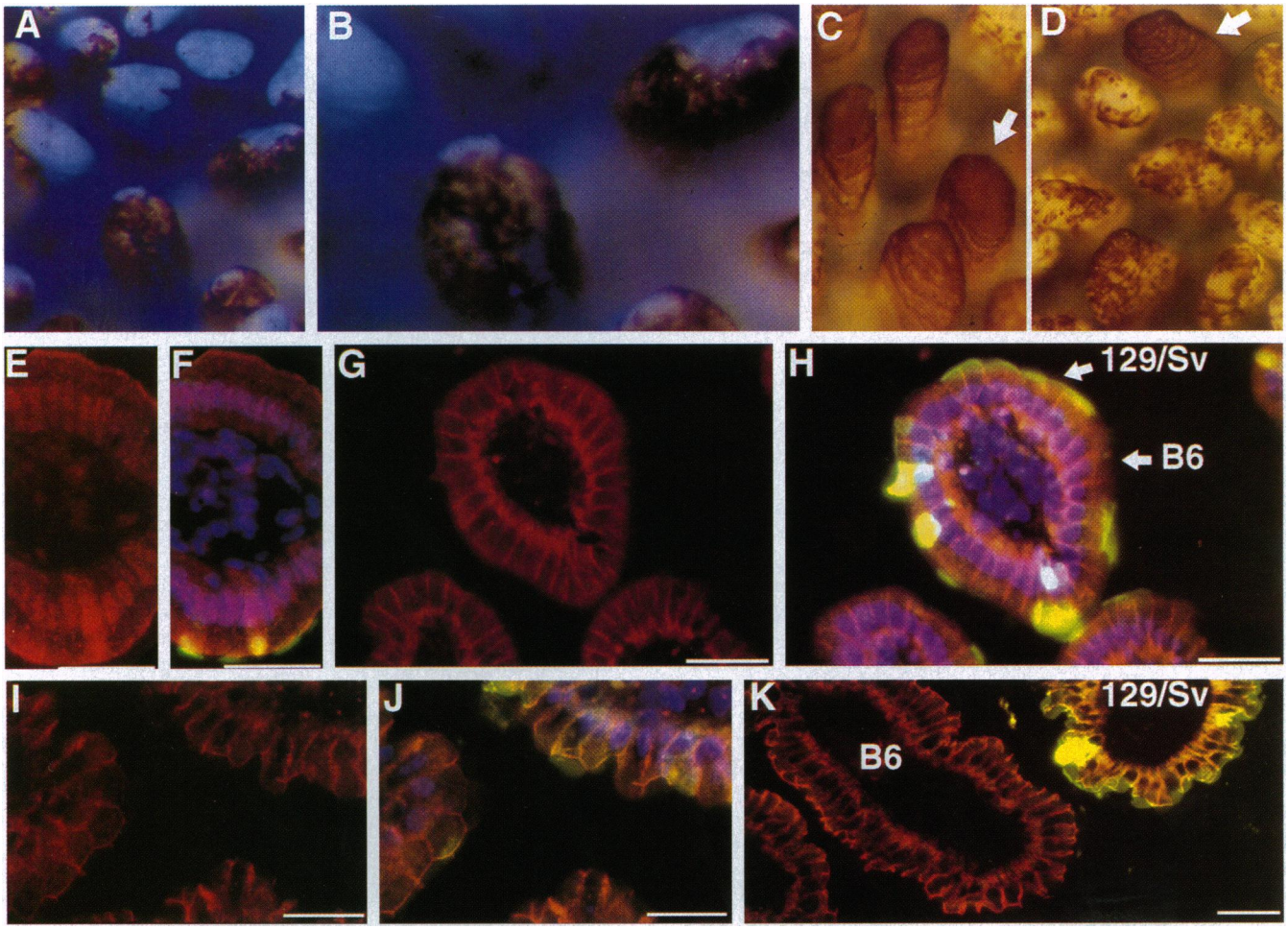

FIG. 2. Forced expression of APC in B6-ROSA26 ↔ 129/Sv-APC^{Wt} chimeric transgenic mice disrupts the orderliness of cell migration. (*A* and *B*) Jejunal whole mount from a 1.5-month-old B6-ROSA26 ↔ 129/Sv-APC^{Wt} chimera stained with X-Gal and peroxidase-UEA1. The whole mount shows polyclonal villi with intermingled and dispersed populations of B6 and 129/Sv epithelial cells. (*C* and *D*) Jejunal whole mount stained with UEA1 alone. The arrows point to villi composed entirely of 129/Sv-APC epithelial cells (arrows). The disordered migration is only evident in the adjacent polyclonal villi where brown UEA1$^+$ 129/Sv-APC^{Wt} cells are dispersed among white B6 cells. (*E* and *F*) Section cut perpendicular to the crypt-villus axis at the midportion of a jejunal villus. The section was incubated with affinity purified rabbit anti-APC (visualized as red with Cy3-donkey anti-rabbit Ig in *E*), fluorescein isothiocyanate (FITC)-conjugated UEA1 (green in *F*) plus bis-benzimide (blue nuclear stain in *F*). Comparison of *E* with the triple exposure of the same section in *F* reveals that 129/Sv-APC epithelial cells (yellow-green apical staining) have higher levels of APC than adjacent nontransgenic B6-ROSA cells. (*G* and *H*) Section of a jejunal villus, oriented as in *E* and *F*, and stained with rabbit anti-α-catenin and Cy3-donkey anti-rabbit Ig (*G*) plus FITC-UEA1, and bis-benzimide (*H*). Comparison of B6 and 129/Sv cells in the polyclonal villus indicates that forced expression of APC^{Wt} does not affect the intracellular distribution of α-catenin. (*I* and *J*) Section processed as in *G* and *H*, except that rabbit anti-β-catenin antibodies were used. No differences in β-catenin compartmentalization are detectable between UEA1$^+$ 129/Sv-APC and UEA1$^-$B6-ROSA26 cells. (*K*) Section of adjacent UEA1$^+$ 129/Sv and UEA1$^-$B6-ROSA26 jejunal villi, incubated with E-cadherin mAbs (detected with Cy3-donkey anti-rat Ig) and FITC-UEA1. Forced expression of APC^{Wt} has no discernible effect on the intracellular distribution of E-cadherin. (Bars = 25 μm.)

likely involves the crypt stem cell or one of its immediate descendants (e.g., refs. 37 and 42). APC^{Wt} appears to be strategically placed at the crypt-villus junction and at the crypt base to influence the orderly bipolar migration of epithelial cells. APC^{Wt} is also present at highest levels in the upper portions of human colonic crypts (43). APC mutations that lead to a decrease in APC–catenin complex formation may allow the opposing activity of cadherin–catenin complexes to predominate, yielding an adhesive migration phenotype and increasing the chances that an initiated cell is entrapped within the crypt. This effect, together with other effects of *APC* gene mutations (e.g., on regulation at the G_0G_1/S boundary of the cell cycle), could increase the likelihood that an initiated cell is able to undergo clonal expansion and acquire the additional genetic alterations needed to complete the multistep journey to neoplasia (44).

The complex intracellular distribution of APC within intestinal epithelial cells (Fig. 1*I*; ref. 34) raises questions about the mechanism(s) by which APC is able to influence cell movement. A polyclonal villus in B6-ROSA26 ↔ 129/Sv-APC mice represents an *in vivo* experiment (129/Sv-APC^{Wt} cells) with its own internal control (B6 cells), where the effects of forced expression of APC^{Wt} on mediators of cell–cell and/or cell–substratum interactions can be examined.

Finally, it is important to point out that lacZ is expressed in the B6 component of developing and adult B6-ROSA26 ↔ 129/Sv stomach plus other organs. The ability to genotype a wide variety of cell populations in chimeric mice generated from B6-ROSA26 blastocysts and genetically manipulated ES cells (including those homozygous for a given null allele) should allow these animals to be used for a large number of loss-of-function or gain-of-function experiments.

We thank David O'Donnell, Chandra Oleksiewicz, and Maria Karlsson for superb technical assistance. This work was supported in part by National Institutes of Health Grants DK37960 and DK30292.

1. Joslyn, G., Carlson, M., Thliveris, A., Albertsen, H., Gelbert, L., *et al.* (1991) *Cell* **66,** 601–613.
2. Groden, J., Thliveris, A., Samowitz, W., Carlson, M., Gelbert, L., *et al.* (1991) *Cell* **66,** 589–600.
3. Kinzler, K., Nilbert, M., Vogelstein, B., Bryan, T., Levy, D., Smith, K., Preisinger, A., Hamilton, S., Hedge, P., Markham, A., Carlson, M., Joslyn, G., Groden, J., White, R., Miki, Y., Miyoshi, Y., Nishisho, I. & Nakamura, Y. (1991) *Science* **251,** 1366–1370.
4. Polakis, P. (1995) *Curr. Opin. Genet. Dev.* **5,** 66–71.
5. Nishisho, I., Nakamura, Y., Miyoshi, Y., Miki, Y., Ando, H., *et al.* (1991) *Science* **253,** 665–669.
6. Hamilton, S. R., Liu, B., Parsons, R. E., Papadopoulos, N., Jen, J., *et al.* (1995) *N. Engl. J. Med.* **332,** 839–847.
7. Su, L.-K., Kinzler, K. W., Vogelstein, B., Preisinger, A. C., Moser, A. R., Luongo, C., Gould, K. A. & Dove, W. F. (1992) *Science* **256,** 668–670.
8. Dove, W. F., Luongo, C., Connelly, C. S., Gould, K. A., Shoemaker, A. R., Moser, A. R. & Gardner, R. L. (1994) *Cold Spring Harbor Symp. Quant. Biol.* **59,** 501–508.
9. Luongo, C., Moser, A. R., Gledhill, S. & Dove, W. F. (1994) *Cancer Res.* **54,** 5947–5952.
10. Moser, A. R., Shoemaker, A. R., Connelly, C. S., Clipson, L., Gould, K. A., Luongo, C., Dove, W. F., Siggers, P. H. & Gardner, R. L. (1995) *Dev. Dyn.* **203,** 422–433.
11. Smith, K. J., Levy, D. B., Maupin, P., Pollard, T. D., Vogelstein, B. & Kinzler, K. W. (1994) *Cancer Res.* **54,** 3672–3675.
12. Munemitsu, S., Souza, B., Müller, O., Albert, I., Rubinfeld, B. & Polakis, P. (1994) *Cancer Res.* **54,** 3676–3681.
13. Nagafuchi, A. & Takeichi, M. (1988) *EMBO J.* **7,** 3679–3684.
14. Ozawa, M., Barbibault, H. & Kemler, R. (1989) *EMBO J.* **8,** 1711–1717.
15. Hermiston, M. L. & Gordon, J. I. (1995) *J. Cell Biol.* **129,** 489–506.
16. Hinck, L., Näthke, I. S., Papkoff, J. & Nelson, W. J. (1994) *J. Cell Biol.* **125,** 1327–1340.
17. Watabe, M., Nagafuchi, A., Tsukita, S. & Takeichi, M. (1994) *J. Cell Biol.* **127,** 247–256.
18. Rubinfeld, B., Souza, B., Albert, I., Muller, O., Chamberlain, S. H., Masiarz, F. R., Munemitsu, S. & Polakis, P. (1993) *Science* **262,** 1731–1734.
19. Su, L-K., Vogelstein, B. & Kinzler, K. W. (1993) *Science* **262,** 1734–1737.
20. Rubinfeld, B., Souza, B., Albert, I., Munemitsu, S. & Polakis, P. (1995) *J. Biol. Chem.* **270,** 5549–5555.
21. Papkoff, J., Rubinfeld, B., Schryver, B. & Polakis, P. (1996) *Mol. Cell. Biol.* **16,** 2128–2134.
22. Rubinfeld, B., Albert, I., Porfiri, E., Fiol, C., Munemitsu, S. & Polakis, P. (1996) *Science* **272,** 1023–1026.
23. Munemitsu, S., Albert, I., Souza, B., Rubinfeld, B. & Polakis, P. (1995) *Proc. Natl. Acad. Sci USA* **92,** 3046–3050.
24. Gordon, J. I. & Hermiston, M. L. (1994) *Curr. Opin. Cell Biol.* **6,** 795–803.
25. Bry, L., Falk, P., Huttner, K., Ouellette, A., Midtvedt, T. & Gordon, J. I. (1994) *Proc. Natl. Acad. Sci. USA* **91,** 10335–10339.
26. Hermiston, M. L., Green, R. P. & Gordon, J. I. (1993) *Proc. Natl. Acad. Sci. USA* **90,** 8866–8870.
27. Hermiston, M. L. & Gordon, J. I. (1995) *Science* **270,** 1203–1207.
28. Friedrich, G. & Soriano, P. (1991) *Genes Dev.* **5,** 1513–1523.
29. McLean, I. W. & Nakane, P. K. (1974) *J. Histochem. Cytochem.* **22,** 1077–1083.
30. Hermiston, M. L., Wong, M. H. & Gordon, J. I. (1996) *Genes Dev.* **10,** 985–996.
31. Näthke, I. S., Hinck, L., Swedlow, J. R., Papkoff, J. & Nelson, W. J. (1994) *J. Cell Biol.* **125,** 1341–1352.
32. Vestweber, D. & Kemler, R. (1985) *EMBO J.* **4,** 3393–3398.
33. Hall, P. A., Coates, P. J., Ansari, B. & Hopwood, D. (1994) *J. Cell. Sci.* **107,** 3569–3577.
34. Miyashiro, I., Senda, T., Matsumine, A., Baeg, G. H., Kuroda, T., Shimano, T., Miura, S., Noda, T., Kobayashi, S. & Monden, M. (1995) *Oncogene* **11,** 89–96.
35. Peifer, M. (1996) *Science* **272,** 974–975.
36. Trahair, J., Neutra, M. & Gordon, J. I. (1989) *J. Cell Biol.* **19,** 3231–3242.
37. Kim, S. H., Roth, K. A., Moser, A. R. & Gordon, J. I. (1993) *J. Cell Biol.* **123,** 877–893.
38. Baeg, G.-H., Matsumine, A., Kuroda, T., Bhattacharjee, R. N., Miyashiro, I., Toyoshima, K. & Akiyama, T. (1995) *EMBO J.* **14,** 5618–5625.
39. Joslyn, G., Richardson, D. W., White, R. & Alber, T. (1993) *Proc. Natl. Acad. Sci. USA* **90,** 11109–11113.
40. Frisch, S. M. & Francis, H. (1994) *J. Cell Biol.* **124,** 619–626.
41. Ruoslahti, E. & Reed, J. C. (1994) *Cell* **7,** 477–478.
42. Moser, A. R., Dove, W. F., Roth, K. A. & Gordon, J. I. (1992) *J. Cell Biol.* **116,** 1517–1526.
43. Smith, K. J., Johnson, K. A., Bryan, T. M., Hill, D. E. Markowitz, S., Wilson, J. K. V., Paraskeva, C., Petersen, G. M., Hamilton, S. R., Vogelstein, B. & Kinzler, K. W. (1993) *Proc. Natl. Acad. Sci. USA* **90,** 2846–2850.
44. Fearon, E. R. & Vogelstein, B. (1990) *Cell* **61,** 759–767.